Organic Microlaser Based on Aggregation-Induced Emission Fluorophores for Tensile Strain Sensing

Xiaoping Guo[1], Shijie Zhen[2], Tianchang Ouyang[1], Shangxiong Zhou[3], Qiwen Pan[1], Dandan Yang[1], Jianhao Chen[1], Guoping Dong[1], Zujin Zhao[2*], Jianrong Qiu[4], and Ben Zhong Tang[2,5]*

1 State Key Laboratory of Luminescent Materials and Devices, and Guangdong Provincial Key Laboratory of Fiber Laser Materials and Applied Techniques, and Guangdong Engineering Technology Research and Development Center of Special Optical Fiber Materials and Devices, School of Materials Science and Engineering, South China University of Technology, Guangzhou 510640, China

2 State Key Laboratory of Luminescent Materials and Devices, Guangdong Provincial Key Laboratory of Luminescence from Molecular Aggregates, SCUT-HKUST Joint Research Institute, South China University of Technology, Guangzhou 510640, China

3 Institute of Polymer Optoelectronic Materials and Devices, State Key Laboratory of Luminescent Materials and Devices, South China University of Technology, Guangzhou 510640, China

4 College of Optical Science and Engineering, State Key Laboratory of Modern Optical Instrumentation, Zhejiang University, Hangzhou 310027, China

5 Department of Chemistry, The Hong Kong University of Science & Technology, Clear Water Bay, Kowloon, Hong Kong, China.

Supplementary Information

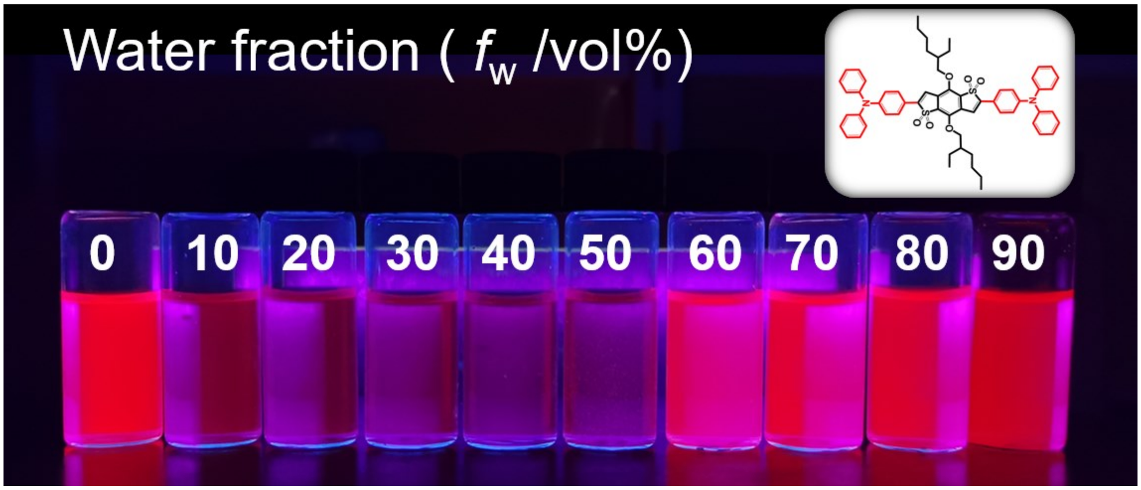

Figure S1. The optical images of TPA-BDTO in water/THF mixtures with different f_ws under 365nm UV light; (insert) the chemical structure of TPA-BDTO. Optical images reflect the emission variations of TPA-BDTO more intuitively.

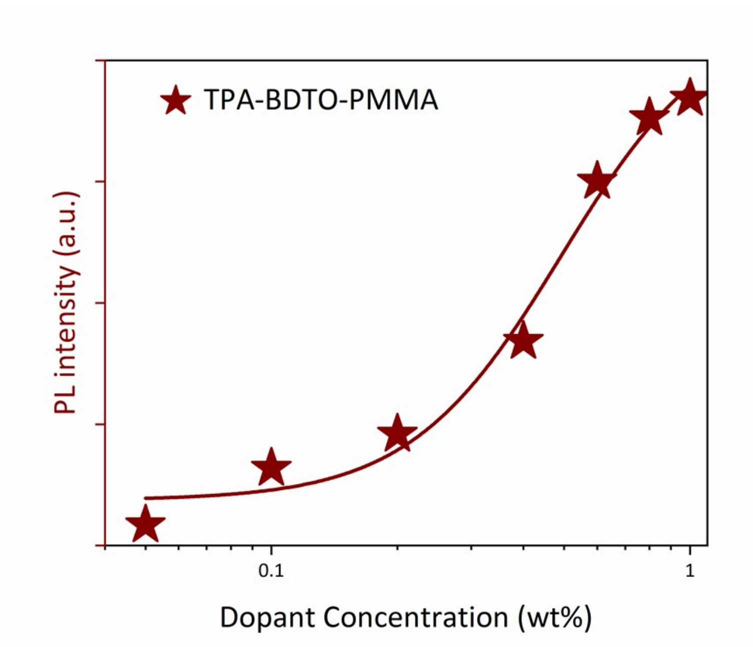

Figure S2. The PL intensity of TPA-BDTO-PMMA mixture with various doping concentration. With the increasing concentration (weight percentage of TPA-BDTO and PMMA, wt%) of TPA-BDTO, the precursor materials TPA-BDTO-PMMA show growing photoluminescence (PL) intensity. To this end, the limitation of concentration quenching problem is broken.

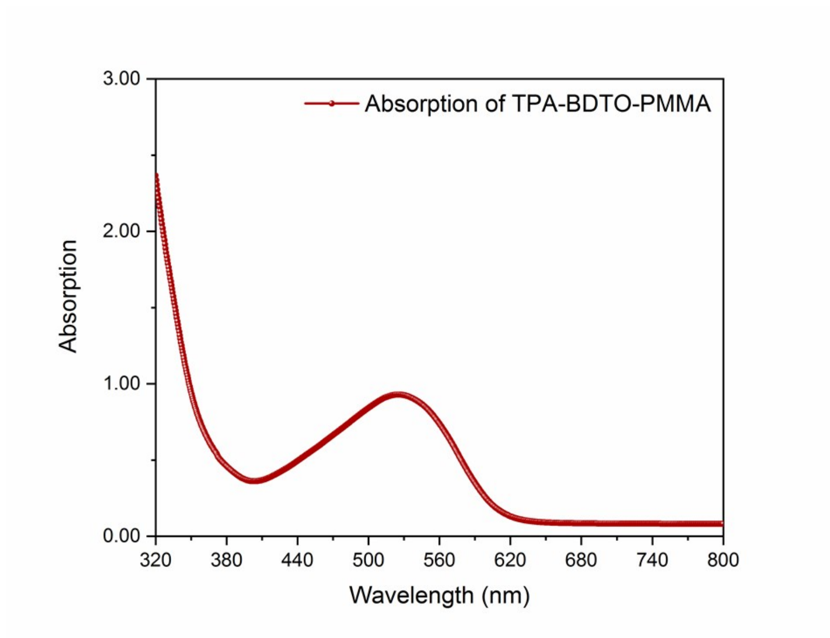

Figure S3. The absorption spectrum of TPA-BDTO-PMMA. The position of absorption peak directly characterized by spectrophotometer is consistent with the peak position of transmission spectrum in Fig. 1, which confirms that TPA-BDTO-PMMA has less light scattering and further reduces the optical loss.

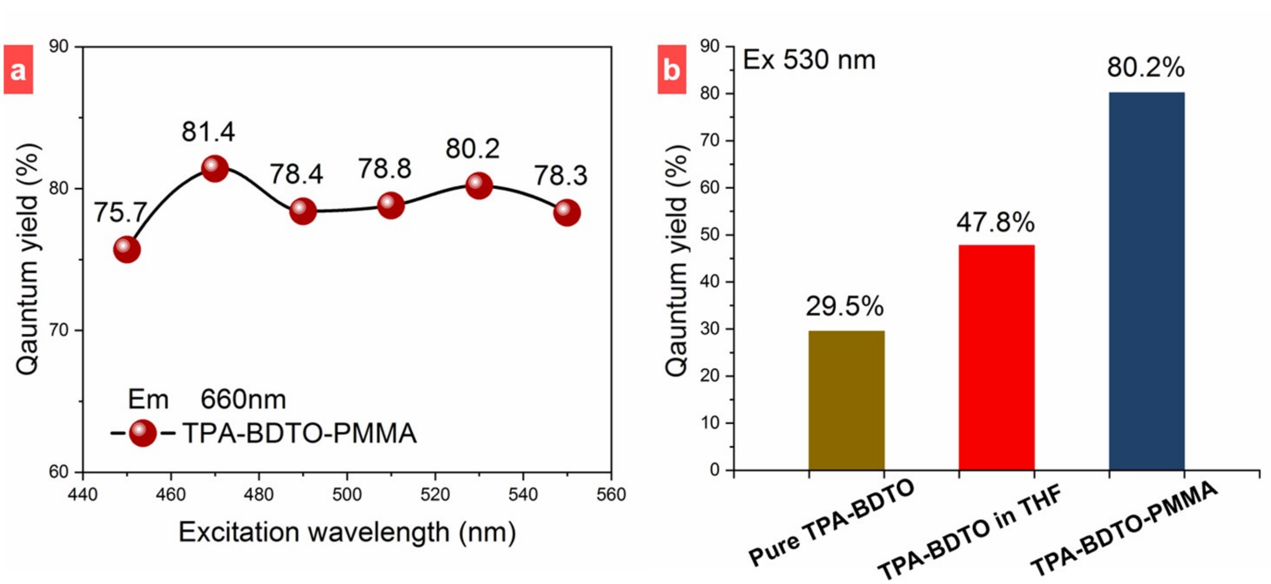

Figure S4. The PLQYs of the materials used for the microlaser. (a) The PLQYs of TPA-BDTO-PMMA at the excitation from 450 nm to 530 nm; (b) The comparison of PLQYs of pure TPA-

BDTO, TPA-BDTO in THF, and TPA-BDTO-PMMA at the same excitation. Thereinto, the PLQYs of TPA-BDTO and TPA-BDTO in THF have been characterized in our previous work.[1]

Table S1. The elasticity modulus of the precursor materials PMMA and TPA-BDTO-PMMA are recorded, comparing with several common materials of traditional microresonators.

Materials	Elasticity modulus (GPa)
Materials PMMA	4.71
TPA-BDTO-PMMA	5.18
Borosilicate glass	69.32
Germanate glass	71.01
Silica glass	72.40
High borosilicate glass	73.40

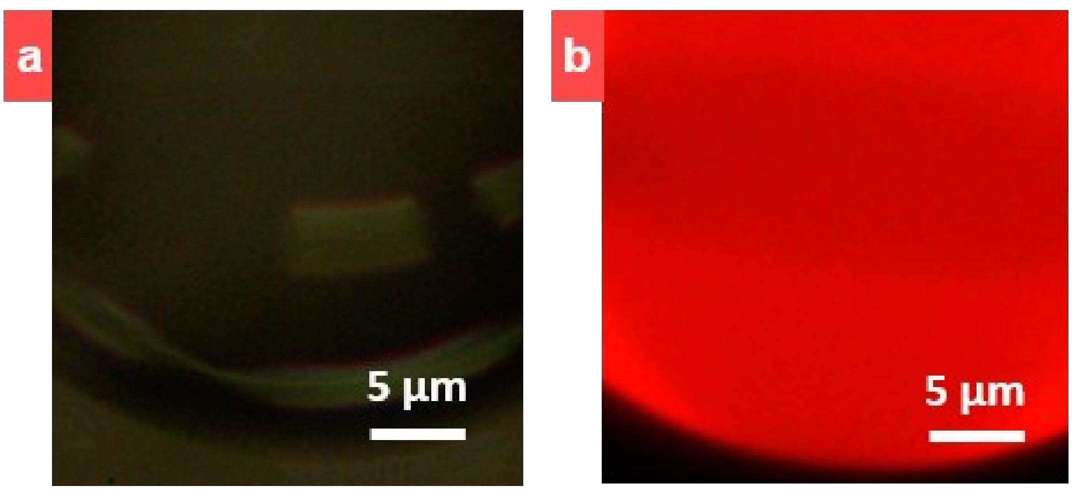

Figure S5. The fluorescence photomicrograph of PMMA microbottle without (a) and with (b) TPA-BDTO. The scale bar is 5 μm. Through a home-made confocal microscope system, nanopulsed laser with 530 nm is focused on the prepared TPA-BDTO-PMMA microbottle. It can be observed that the microbottles containing TPA-BDTO are uniformly red, indicating that TPA-BDTO is evenly distributed in the microresonator.

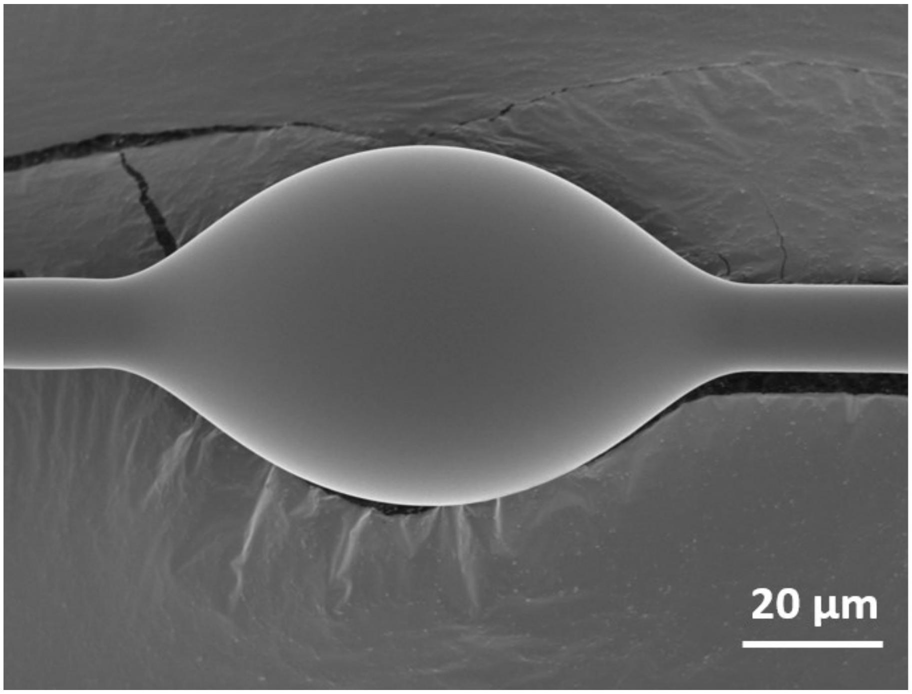

Figure S6. The scanning electron microscope (SEM) image of the prepared microbottle via self-assembly method. Driven by the surface tension, the self-assembled microbottles possess smooth surface, greatly reducing the optical loss during resonance process.

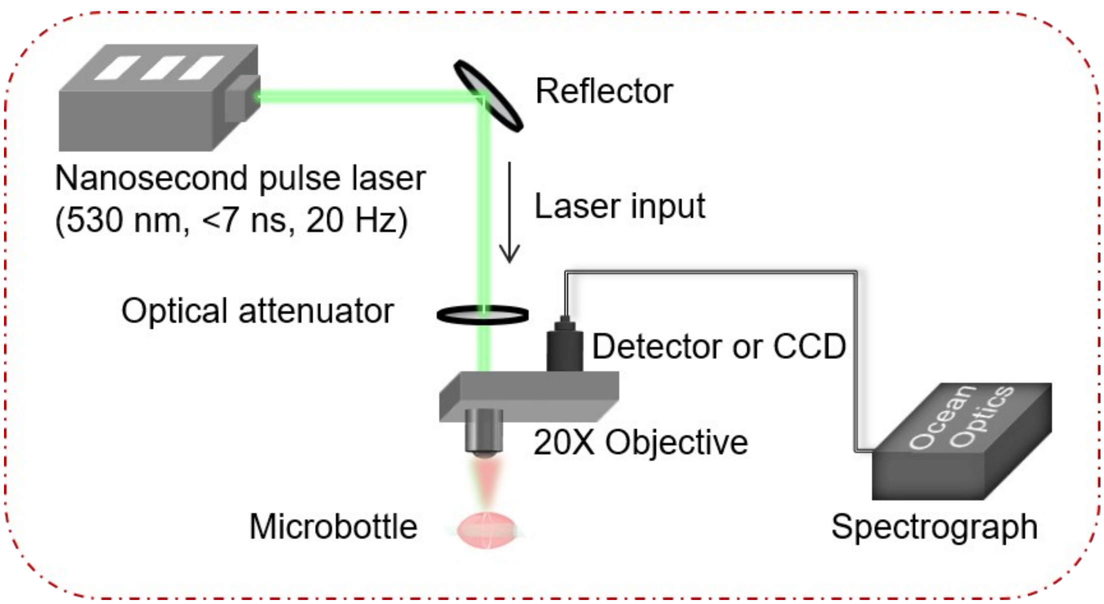

Figure S7. The home-made confocal microscope system for recording the output lasing from TPA-BDTO-PMMA bottle microresonators. The system consists of a pump laser, confocal microscope with 20X objective, a CCD and a spectrometer. The confocal microscope collects the emission from microbottle while focusing the pump laser on it.

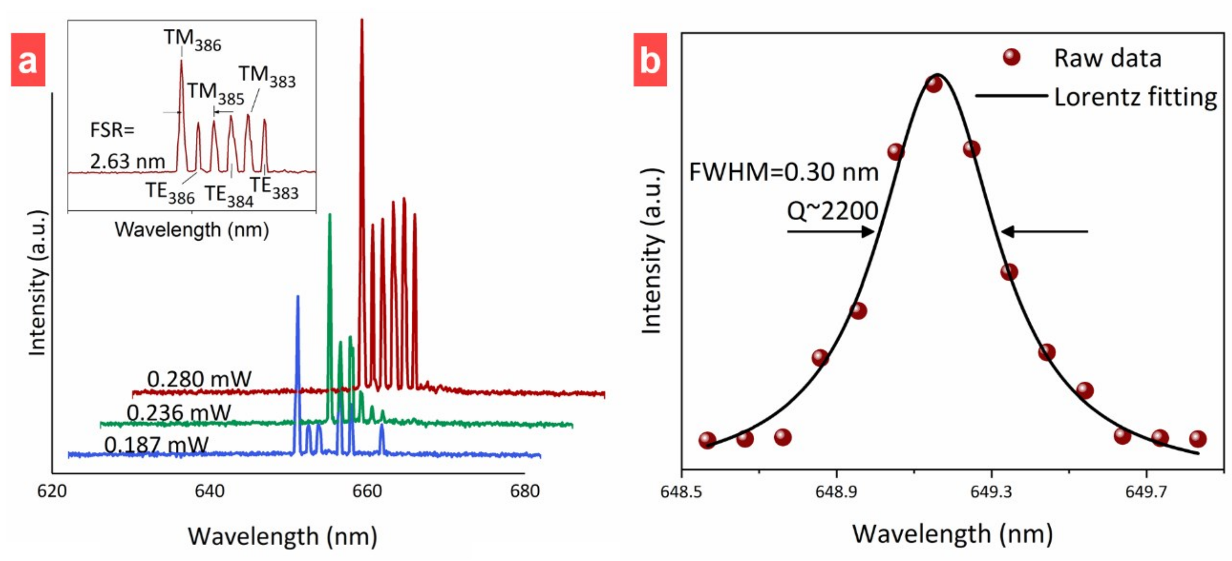

Figure S8. (a) Multi-mode laser of TPA-BDTO doped microbottle with different pump laser power, the left insert illustrates the mode number of the output laser with m = 383-386; (b) The Q factor of a narrow laser peak at 649.15 nm fitting with the Lorentz function.

The intensity of the fundamental mode around 649 nm strongly increases when pump power above 0.187 mW; meanwhile, new sharp peaks emerged from adjacent modes, which is owing to transition from spontaneous emission to stimulated emission.[2] The resonances contain transverse electric (TE) modes and transverse magnetic (TM) modes (insert).[3] The mode number can be calculated in equation (1) [4-6]:

$$\lambda^{-1}(D,n,n_r,r,m) = [\frac{1}{2} + 2^{-\frac{1}{3}}\alpha(r)(m+\frac{1}{3})^{\frac{1}{3}} - \frac{l}{(n_r^2-1)^{\frac{1}{2}}} + \frac{3}{10}2^{\frac{2}{3}}\alpha^2(r)(m+\frac{1}{2})^{-\frac{1}{3}} - 2^{-\frac{1}{3}}\left(n_r^2 - \frac{2}{3}l^2\right)\frac{\alpha(r}{} \quad (1)$$

Where D is the resonance diameters of microbottle, n represents the effective refractive index of the microcavity, n’ donates the environment refractive index, n_r satisfies the equation $n_r = n/n'$, r is the radial mode number, m is specific to the angular mode, and l is the resonance circumference. In TE modes l = n', and in TM modes l = 1/n'. And according to equation (2), we discern that the free spectral range (FSR) between peak TM_{386} and TM_{385} is 2.62 nm, which is similar to the measured results in Figure 3d.

$$FSR = \frac{\lambda^2}{\pi D n} \quad (2)$$

Picking up the narrow laser peak at 649.15 nm with a FWHM of 0.30 nm (Figure S6b), the microlaser presents good fitting with Lorentz function, which exerts a high Q factor of about 2200 with the relationship $Q = \lambda/\lambda_{FWHM}$.

Table S2. The refractive index of the cavity materials PMMA and TPA-BDTO-PMMA.

Sampling points	1	2	3	4	5	Average
PMMA	1.4897	1.4894	1.4895	1.4897	1.4896	1.4896
TPA-BDTO-PMMA	1.4887	1.4882	1.4887	1.4892	1.4889	1.4887

Here, PMMA and TPA-BDTO-PMMA was made into a wafer with the thickness of 2 mm. To ensure that the refractive index is accurately measured, we selected five points on the sample for testing, and finally calculated the average.

Table S3. The performance comparison of various strain detection sensors.

Sensors	Sensitivity or Gauge factor	Reference
Graphene foam/PDMS stretchable strain sensor	2.2	7

Carbon based Ecoflex stretchable strain sensor	3.8	8
PDMS microsphere force sensor	1 pm μN^{-1}	9
PDMS WGM microresonator gravity sensor	22.74 ± 6.87 pm μN^{-1}	10
GaN WGM microlasing straing sensor	0.15 pm $\mu\varepsilon^{-1}$	11
TPA-BDTO-PMMA microbottle axial tensile strain sensor	0.34 pm $\mu\varepsilon^{-1}$	This work

Supplementary movie 1: The process of lasing output from TPA-BDTO-PMMA microbottle with the pump power increasing.

Supplementary movie 2: A schematic animation of axial tension strain sensing and recovery process.

REFERENCES

1 S. Zhen, S. Wang, S. Li, W. Luo, M. Gao, L. G. Ng, C. C. Goh, A. Qin, Z. Zhao and B. Liu, *Adv. Funct. Mater.*, 2018, **28**, 1706945.

2 C. Wei, Y. X. Du, Y. Y. Liu, X. Q. Lin, C. Zhang, J. N. Yao and Y. S. Zhao, *J. Am. Chem. Soc.*, 2019, **141**, 5116-5120.

3 A. N. Oraevsky, Quantum Electronics, 2002, **32**, 377-400.

4 V. D. Ta, R. Chen, D. M. Nguyen and H. D. Sun, Appl. Phys. Lett., 2013, **102**, 4.

5 V. D. Ta, R. Chen, L. Ma, Y. J. and Ying, H. D. Sun, Laser & Photonics Reviews, 2013, **7**, 133-139.

6 R. Chen, V. D. Ta and H. D. Sun, ACS Photonics, 2014, **1**, 11-16.

7 Y. R. Jeong, H. Park, S. W. Jin, S. Y. Hong, S. S. Lee and J. S. Ha, Adv. Funct. Mater., 2015, **25**, 4228-4236.

8 J. T. Muth, D. M. Vogt, R. L. Truby, Y. Menguec, D. B. Kolesky, R. J. Wood and J. A. Lewis, Adv. Mater., 2014, **26**, 6307-6312.

9 T. Ioppolo, U. K. Ayaz and M. V. Otugen, J. Appl. Phys., 2009, **105**, 013535.

10 Z. H. Zhou, F. J. Shu, Z. Shen, C. H. Dong and G. C. Guo, Sci. China Phys. Mech., 2015, **58**, 114208.

11 Y. Y. Peng, J. F. Lu, D. F. Peng, W. D. Ma, F. T. Li, Q. S. Chen, X. D. Wang, J. L. Sun, H. T. Liu and C. F. Pan, Adv. Funct. Mater., 2019, **29**, 1905051.